



HAL
open science

Fine particulate matter exposure and health impacts from indoor activities

Rachna Bhoonah, Alice Maury-Micolier, Olivier Jolliet, Peter Fantke

► **To cite this version:**

Rachna Bhoonah, Alice Maury-Micolier, Olivier Jolliet, Peter Fantke. Fine particulate matter exposure and health impacts from indoor activities. *Indoor Air*, 2023, 10.1155/2023/8857446 . hal-04266664

HAL Id: hal-04266664

<https://hal.science/hal-04266664>

Submitted on 31 Oct 2023

HAL is a multi-disciplinary open access archive for the deposit and dissemination of scientific research documents, whether they are published or not. The documents may come from teaching and research institutions in France or abroad, or from public or private research centers.

L'archive ouverte pluridisciplinaire **HAL**, est destinée au dépôt et à la diffusion de documents scientifiques de niveau recherche, publiés ou non, émanant des établissements d'enseignement et de recherche français ou étrangers, des laboratoires publics ou privés.

1 **Fine particulate matter exposure and health impacts from indoor activities**

2 Rachna Bhoonah^{a*}, Alice Maury-Micolier^b, Olivier Jolliet^{c, d} and Peter Fantke^{c*}

3

4 ^aMines Paris-PSL, CES – Center for Energy Efficiency of Systems, 60 Bd St Michel, 75006
5 Paris, France

6 ^bOctopus Lab, 237 Rue du Ballon, 59110 La Madeleine, France

7 ^cQuantitative Sustainability Assessment, Department of Environmental and Resource
8 Engineering, Technical University of Denmark, Bygningstorvet 115, 2800 Kgs. Lyngby,
9 Denmark

10 ^dEnvironmental Health Sciences, School of Public Health, University of Michigan, Ann Arbor,
11 MI 48109, USA

12 ORCID

13 Rachna Bhoonah: <https://orcid.org/0000-0002-9476-4014>

14 Alice Maury-Micolier: <https://orcid.org/0000-0002-4615-1205>

15 Olivier Jolliet: <https://orcid.org/0000-0001-6955-4210>

16 Peter Fantke: <http://orcid.org/0000-0001-7148-6982>

17

18 *Corresponding author: E-mail: pefan@dtu.dk.

19 *Co-corresponding author: E-mail: rachna.bhoonah@minesparis.psl.eu.

20

21 **Abstract**

22 Exposure to fine particulate matter (PM_{2.5}) is an important contributor to global human
23 disease burden, particularly indoors where people spend the majority of their time and exposure
24 is highest. We propose a framework linking indoor PM_{2.5} emissions from human activities to
25 exposure and health impacts, expressed in Disability-Adjusted Life Years (DALY). Derived
26 dynamic indoor PM_{2.5} concentrations—capturing temporal variations through different window
27 opening scenarios and air renewal rates—are used to estimate uncertainty for a parametric
28 model (up to a factor 114). Intake fractions (fraction of emitted substance taken in,
29 $\mu\text{g}_{\text{intake}}/\mu\text{g}_{\text{emitted}}$), effect factors ($\mu\text{DALY}/\mu\text{g}_{\text{intake}}$), related impact characterisation factors (health
30 impact per unit mass emitted, $\mu\text{DALY}/\mu\text{g}_{\text{emitted}}$) and impact scores (health impact per hour
31 activity, $\mu\text{DALY}/\text{h}_{\text{activity}}$) are provided for 19 one-hour indoor activities, and can be flexibly
32 scaled to real activity durations. Indoor concentrations exceeded recommended World Health
33 Organization (WHO) limits for all activities at low ventilation rates. Per person, 98 to
34 $119 \mu\text{DALY}/\text{h}_{\text{activity}}$ (52 to 63 $\text{minutes}_{\text{lost}}/\text{h}_{\text{activity}}$) were associated with traditional fuel cook
35 stoves, with high air renewal rates (3 and 14 h^{-1}). The burning of candles, at low air renewal
36 rates of 0.2 to 0.6 h^{-1} , results in 7 to $11 \mu\text{DALY}/\text{h}_{\text{activity}}$ (4 to 11 $\text{minutes}_{\text{lost}}/\text{h}_{\text{activity}}$). Derived
37 impact scores and characterisation factors serve as a starting point for integrating indoor PM_{2.5}
38 emissions and exposure into life cycle impact and public health assessments.

39 **Keywords:** indoor air quality, life cycle assessment, air pollution, PM_{2.5}, cook stove

40

41 **Synopsis**

42 Exposure to indoor PM_{2.5} is lacking in existing impact calculation methods. This paper
43 shows that indoor exposure can be above recommended values, and provides impact scores for
44 19 common indoor activities.

45 **1. Introduction**

46 Ambient and household fine particulate matter (PM_{2.5}) pollution is one of the major
47 global health risk factors, representing 120 million and 92 million Disability-Adjusted Life
48 Years (DALYs) each in 2019 (4.7% and 3.6% of total DALYs) [1]. Serious health outcomes
49 are associated with PM_{2.5} exposure, including chronic obstructive diseases (COPD), ischemic
50 heart disease (IHD), stroke and lung cancer (LC) for adults, and acute lower respiratory diseases
51 (ALRI) for children who are still in the developmental stage (< 5 years) [2,3]. Indoor
52 environments, where people spend a high fraction of their time, are particularly important to
53 study: 83% to 90% of exposure occurs indoors [4]. Since buildings have relatively small,
54 enclosed volumes, indoor air concentrations can be particularly high as compared to ambient
55 levels. For instance, PM_{2.5} air concentrations were higher than the World Health Organization's
56 (WHO) annual guideline values in schools and kindergartens by a factor 4 to 15 [5–7].
57 According to these guidelines, annual exposures should remain below 5 µg/m³, and 24-hour
58 exposures can exceed 15 µg/m³ for no more than 3 to 4 days per year [8]. Inhabitants of rural
59 areas, especially in developing countries, are particularly at risk due to wide usage of solid fuel
60 combustion indoors for cooking or heating [9–11].

61 Indoor PM_{2.5} concentrations depend on outdoor pollution levels, penetrating through
62 unfiltered ventilation, indoor primary emissions from activities, and chemical reactions
63 between substances such as the oxidation of volatile organic compounds (VOCs) with ozone,
64 nitrate and hydroxyl radicals which can form secondary PM [12]. Various studies have
65 measured primary PM_{2.5} emission rates, indoor concentrations and particle size distributions
66 [15–23] for different activities. While fuel stoves are recognised as strong indoor PM_{2.5} sources
67 and linked to premature mortality in developing countries, cooking (especially frying and
68 grilling) and candle burning were also identified as important sources. Occupant contributions
69 to indoor PM_{2.5} from the shedding of skin and cloth fibres or the resuspension of particles during

70 activities [24–28] have also been measured, and are highly dependent on dust coverage and,
71 ultimately, occupant behaviour (e.g. frequency of cleaning or presence in dusty environments).
72 Indoor concentrations are affected by air changes per hour (ACH), the presence of filters for
73 mechanical ventilation, and the size and orientation of windows for natural ventilation.

74 Human health impacts of products from outdoor PM_{2.5} emissions can be calculated
75 using life cycle assessment (LCA), a tool used to evaluate the environmental performance of
76 products and technologies over their life cycles, considering different impact categories. The
77 UNEP/SETAC Life Cycle Initiative identified the PM_{2.5} impact category as one of the
78 categories requiring refinements [3]. These include the need for representative indoor
79 archetypes treating indoor sources of PM_{2.5} and consequent occupant exposures.

80 Archetypes have been defined by Fantke et al. [4] according to parameters identified by
81 Hodas et al. [29], including air renewal rates and occupancy. Parametric models coupled with
82 these indoor archetypes can provide average PM_{2.5} concentrations and intake fractions (mass
83 taken in per unit mass emitted) [4], but usually do not capture temporal variations in emission
84 or ventilation rates. Dynamic simulations, using airflow simulation tools such as CONTAM
85 (used by INCA-Indoor [30]) or COMIS, can provide full concentration/exposure profiles that
86 can be coupled with effect factors to calculate health impacts. There is still, however, a need
87 for defining emission scenarios linked to indoor sources and their emission rates. In addition,
88 factors linking emissions, exposure and health effects to particular indoor activities are missing
89 in LCA literature. To address this gap, our study aims to propose a framework for characterising
90 human exposure to PM_{2.5} and related health impacts associated with common indoor activities
91 and their emissions. To achieve this aim, we will address the following three specific objectives:

- 92 1. Propose a framework for linking human indoor activities to primary PM_{2.5}
93 emissions, exposure, effects and health damage based on a dynamic modelling
94 approach,

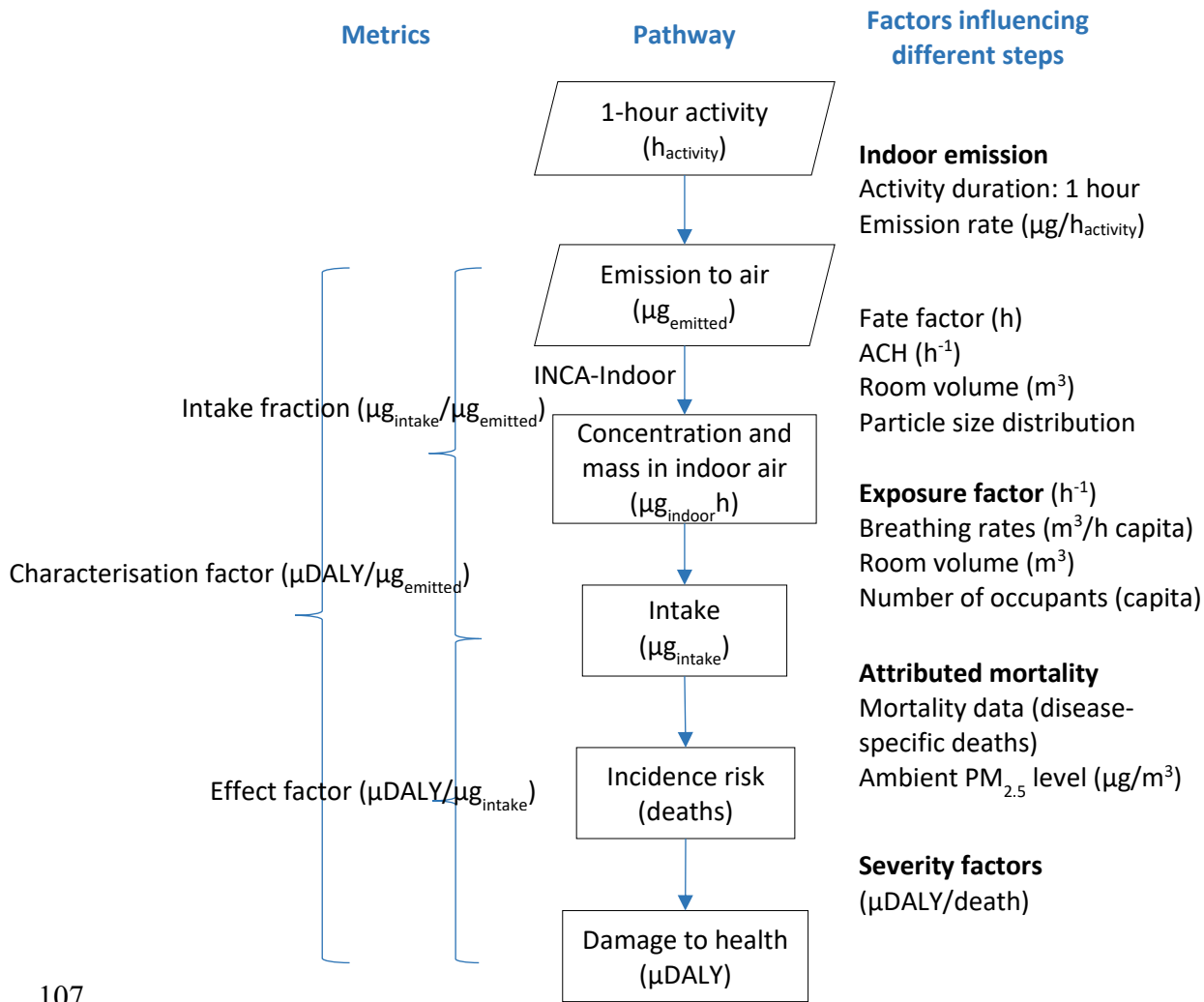
- 95 2. Calculate dynamic indoor PM_{2.5} concentrations and derive a parameterised exposure
96 and effect model for integration in life cycle impact assessment, and
97 3. Provide a set of impact characterisation factors for different reference indoor
98 activities under different natural ventilation scenarios.

99 Resuspension and secondary PM_{2.5} are not within the scope of this study, since they
100 depend on dust coverage and the presence of precursors such as VOCs, which are not currently
101 treated by the dynamic model.

102 **2. Methods**

103 **2.1. Overall followed source-to-damage approach**

104 The pollutant pathway from emission to impact is modelled using the framework
105 recommended in global consensus-building efforts for PM_{2.5} exposure and effects [3,31],
106 adapted to indoor contexts (Figure 1). The functional unit is defined as one hour of activity.



107

108 **Figure 1: Framework for the calculation of activity impact scores from PM_{2.5} emission rates.**

109 Indoor PM_{2.5} concentrations C_{in} ($\mu\text{g}/\text{m}^3$) are simulated with INCA-Indoor, considering

110 1) indoor emission rates of different activities $\dot{m}_{\text{emitted in,avg}}$ ($\mu\text{g}_{\text{emitted}}/h_{\text{activity}}$) obtained from

111 studies, 2) the penetration from outdoors with natural ventilation $\dot{m}_{\text{penetration,avg}}$ ($\mu\text{g}/h$) (5) and

112 3) air renewal rates (h^{-1}). These are compared to a parametric model's results, using one hour

113 as reference activity duration under multiple given air change rates ACH (h^{-1}). Using a fate

114 factor FF (h) or the dynamic fate model INCA-indoor, we determine the evolution of the indoor

115 PM_{2.5} concentrations and the resulting time integrated mass inside the room air. These masses

116 are then multiplied by the exposure rates (h^{-1}) to yield indoor PM_{2.5} intake fractions iF

117 ($\mu\text{g}_{\text{intake}}/\mu\text{g}_{\text{emitted}}$) (2). These iF s are multiplied by effect factors EF ($\mu\text{DALY}/\mu\text{g}_{\text{intake}}$) to obtain

118 the characterisation factors CF ($\mu\text{DALY}/\mu\text{g}_{\text{emitted}}$), i.e. the impact per unit of $\text{PM}_{2.5}$ emitted.
 119 Impact scores IS ($\mu\text{DALY}/\text{h}_{\text{activity}}$) for one person are then calculated as the product of the
 120 cumulative indoor emission $m_{\text{emitted in}}$ ($\mu\text{g}_{\text{emitted}}$) and CF s. This can therefore be expressed as:

$$IS_{\text{activity}} = EF \times iF \times m_{\text{emitted in}} = CF \times m_{\text{emitted in}} \quad (1)$$

121 With

$$iF = \frac{\int_{t=0}^{\infty} BR \times POP \times C_{\text{in,inc}} dt}{m_{\text{emitted in}}} \quad (2)$$

122 Where POP (cap) is the number of occupants, BR is the breathing rate of an occupant
 123 ($\text{m}^3/\text{cap}/\text{h}$). $C_{\text{in,inc}}(t)$ is the increase in indoor $\text{PM}_{2.5}$ concentration due to the activity-related
 124 emissions ($\mu\text{g}/\text{m}^3$) integrated up to infinity (in practice up to the time required to entirely
 125 evacuate the particles emitted by the activity). It is given by the difference between indoor
 126 concentration with activity (C_{in} , in $\mu\text{g}/\text{m}^3$) and without (C_{base} , in $\mu\text{g}/\text{m}^3$).

127 The effect factor depends on the average effective indoor concentration \bar{C}_{in} and the
 128 annual average ambient concentration of the region $\bar{C}_{\text{out},r}$ (Cohen et al. 2017, Fantke et al.
 129 2019).

$$EF(\bar{C}_{\text{in}}) = \frac{dM_{\text{PM}_{2.5}}}{dI_{\text{in}}} \times SF_{i,r} \quad (3)$$

$$= \frac{(RR_i(\bar{C}_{\text{in}} + \Delta C_{\text{in}}) - RR_i(\bar{C}_{\text{in}})) \times \frac{M_{i,r}}{RR_i(\bar{C}_{\text{out},r}) \times POP_r} \times SF_{i,r}}{\Delta \bar{C}_{\text{in}} \times BR_{yr}}$$

130 Where $RR_i(-)$ is the relative risk of developing disease i fom exposure to \bar{C}_{in} (see Fantke
 131 et al. 2019), $\Delta \bar{C}_{\text{in}}$ ($\mu\text{g}/\text{m}^3$) is the increment on the exposure-response curve, $M_{i,r}$ (deaths/year)
 132 the annual mortality in region r due to disease i , POP_r (cap) is the population of the region,

133 $SF_{i,r}$ (DALY/death) is the severity factor specific to the region and disease and BR_{yr} ($m^3/year$)
 134 is the breathing rate. The effect factor depends on exposure concentrations and can hence be
 135 different for activities with different emission rates.

136 The EF depends on the average effective indoor concentration \bar{C}_{in} . This can be either
 137 calculated by INCA-Indoor, or as a comparison calculated using Fantke et al. [4], adapted to
 138 consider intake and deposition for outdoor $PM_{2.5}$:

$$\bar{C}_{in} = \frac{(\dot{m}_{emitted\ in,avg} + \dot{m}_{penetration,avg})}{V_{room} \times \left(ACH_{avg} + DR_{avg} + \frac{BR_{avg} \times POP_{avg}}{V_{room}}\right)} \quad (4)$$

139 $\dot{m}_{penetration,avg}$ ($\mu g/h$) is the average penetration rate of $PM_{2.5}$ from outdoors, defined by:

$$\dot{m}_{penetration,avg} = \bar{C}_{out} \times V_{room} \times ACH_{avg} \quad (5)$$

140 \bar{C}_{out} ($\mu g/m^3$) is the average outdoor $PM_{2.5}$ concentration.

141 2.2. Individual Lifetime Risk

142 The total individual lifetime risk \overline{ILR} (DALY/person) represents the number of life years
 143 lost from exposure to $PM_{2.5}$ over a lifetime for each one-hour activity. It is calculated using
 144 equation (6).

$$\overline{ILR} = N_{activity} \times IS_{activity} \quad (6)$$

145 Where $N_{activity}$ is the number of one-hour activities occurring during a lifetime.

146 2.3. Emission data

147 Primary $PM_{2.5}$ emission rates are collected from various studies for 19 activities and are
 148 presented in Table 1.

Table 1: Primary PM_{2.5} emission rates for 19 activities

Activity	PM _{2.5} emission rate (mg/min)	Reference
Candle burning (low)	0.04	Pagels et al. (2009)
Toasting	0.11	He et al. (2004)
Cooking with electric stove (low)	0.11	He et al. (2004)
Candle burning (medium)	0.15	Pagels et al. (2009)
Incense - aromatic (low)	0.16	Lee and Wang (2004)
Gas stove	0.24	He et al. (2004)
Printer (high)	0.28	He et al. (2010)
Frying (low)	0.43	Aquilina and Camilleri (2022)
Grilling (low)	0.62	Aquilina and Camilleri (2022)
Candle with eucalyptus oil diffusion (high)	0.91	He et al. (2004)
Smoking (passive)	0.99	He et al. (2004)
Cook stove (low) ^a	1.2	Du et al. (2021)
Cooking (high, with burning)	1.33	Aquilina and Camilleri (2022)
Frying (high)	2.68	He et al. (2004)
Grilling (high)	2.78	He et al. (2004)
Coal heating stove ^d	3.50	Li et al. (2022)
Incense - traditional (high)	6.21	Lee and Wang (2004)
Cook stove (medium) ^b	7.9	Shen et al. (2020)
Cook stove (high) ^c	120	Du et al. (2021)

150 a. Fugitive emissions (leakage) from cooking with the burning of coal in an iron stove.

151 b. Fugitive emissions from cooking with the burning of wood in a brick stove.

152 c. Fugitive emissions from cooking with the burning of maize straw in a brick stove.

153 d. Emission rate (mg/min) calculated from the emission factor (g/kg), as described in SI.

154 Cook stove emission rates are highest (up to 120 mg/min) and correspond to common
155 practices in certain rural Chinese homes [22]. Model parameters, including reference outdoor
156 PM_{2.5} concentration and air renewal rates are given in the supporting information (SI) section
157 S.1.

158 **2.4. Dynamic indoor PM_{2.5} concentration calculation**

159 Dynamic concentrations are simulated using the INCA-Indoor multizone model [30].
160 The following inputs are necessary for the simulation: 1) building characteristics, including
161 room dimensions, mechanical ventilation rates if any (not considered in this study), window
162 sizes and layout (modelled with the Pleiades software [36]), 2) dynamic outdoor PM_{2.5}
163 concentrations, 3) meteorological data (temperature, wind speed and direction), 3) indoor PM_{2.5}
164 emission rates, 4) time and duration of emissions and 5) particle size distribution. Room
165 volumes of 30 m³ and 67 m³ are considered, corresponding to 12 m² and 27 m² flooring area,
166 respectively which are within the range of average bedrooms and kitchens [37–39]. Air flows
167 are simulated with CONTAM based on the opening of windows, infiltration rates under 4 Pa
168 and meteorological data, considering a constant indoor temperature of 20 °C. Any
169 interconnecting door between rooms is assumed to be closed, while infiltrations and airflows
170 from differences between open versus closed windows are explicitly considered.
171 Concentrations are calculated with a time step of 10 minutes as a function of airflow rates,
172 emission rates, outdoor PM_{2.5} concentrations and deposition rates.

173 The INCA-Indoor model calculates air PM concentrations based on their size
174 distribution, separated into 27 categories of 0.004 μm to 10 μm. Since particle size distributions
175 are only available for some specific activities, we select a more general indoor distribution,
176 irrespective of the emission source [40]. The distributions are provided in SI section S.3.

177 Because the dynamic model allows to capture variations in air renewal rates, scenarios
178 have been defined to evaluate the effect of window opening on concentrations and health

179 impacts for each activity, hence estimating uncertainties of the parametric model. Air change
180 exchange rates (ACH) between indoor and outdoor air are defined according to Fantke et al.
181 [4]. The average ACH for OECD countries is 0.64 ACH [41], while low-end values are around
182 0.2 ACH for airtight buildings [42]. High air change rates are around 3 ACH, and in non-OECD
183 countries, they can reach 14 ACH.

184 Four standard scenarios are defined: windows always **closed** with infiltration rates of
185 0.2 ACH and 0.6 ACH, and windows always **open** with high and very high ventilation rates of
186 3 ACH and 14 ACH respectively. The air change rates indicated are 24-hour averages, but air
187 flows vary during the day for natural ventilation due to changes in wind speed and direction,
188 temperature, and pressure. In the remaining six scenarios, windows are either open **before**,
189 **during** or **after** activity, with high and very high average air renewal rates of 3 ACH and
190 14 ACH. Since windows are open for a limited duration in the last six scenarios (a minimum of
191 one hour allowed by the model), the ACH can be much higher when open in order to reach the
192 target 24-hour average, but do not exceed a reference comfort speed of 1 m/s [43]. Dynamic
193 ACH are illustrated in SI Figure S2. Very high ventilation rates typically correspond to hot or
194 tropical regions, where cross-ventilation is common. The 10 ventilation scenarios are
195 summarised in SI section S.1.

196 **2.5. Exposure model data**

197 The intake fractions for one occupant are calculated using equation (2) for dynamic
198 concentrations using a breathing rate BR of $16 \text{ m}^3/\text{d}$ [29] and an exposure duration of 24 hours.

199 **2.6. Effect (IER) model data**

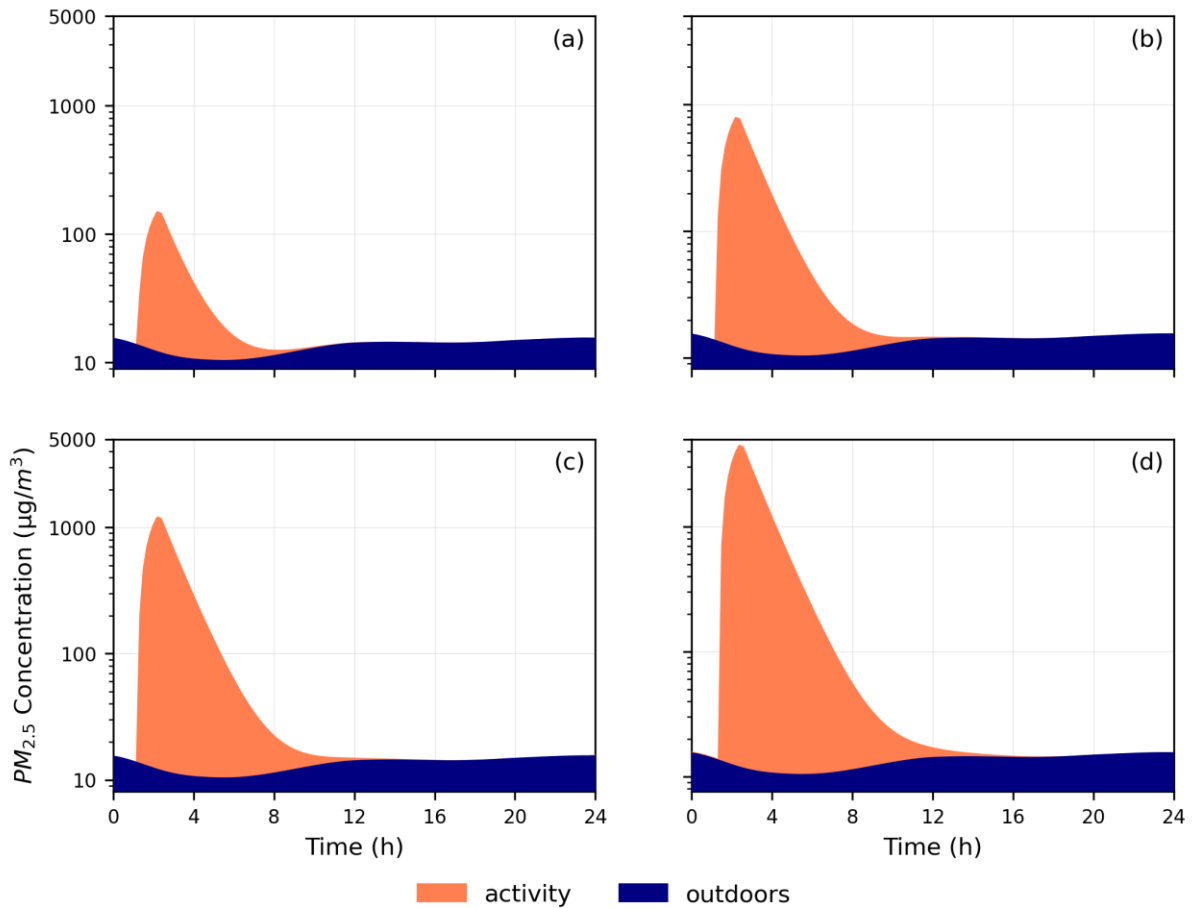
200 Global population data are obtained from world population prospects [44] and age-
201 specific global mortality rates, M (deaths/year), for the five diseases outcomes are obtained
202 from the GBD Collaborative Network for 2019 [45]. An annual average ambient $\text{PM}_{2.5}$ level of

203 16 $\mu\text{g}/\text{m}^3$, corresponding to an average European city [46], is considered and average exposure
204 concentrations \bar{C}_{in} ($\mu\text{g}/\text{m}^3$) are calculated over 24 hours. The calculated effect factor EF only
205 corresponds to exposure to one activity and ambient $\text{PM}_{2.5}$ concentrations, without considering
206 the occurrence of several activities at the same time.

207 **3. Results and discussion**

208 **3.1. Dynamic indoor $\text{PM}_{2.5}$ concentrations**

209 Dynamic $\text{PM}_{2.5}$ concentrations from four indoor activities in a reference room of 30 m^3
210 with closed windows at 0.6 ACH are presented in Figure 2 over 24 hours, a duration that allows
211 to evacuate most activity-related $\text{PM}_{2.5}$ from indoor air. Indoor and outdoor concentrations are
212 dynamic. Indoor concentrations increase after emission, and decrease due to evacuation with
213 air renewal. Outdoor concentrations vary independently of the indoor activity, due to change in
214 outdoor emissions (e.g. fuel burning) or wind speeds.



215

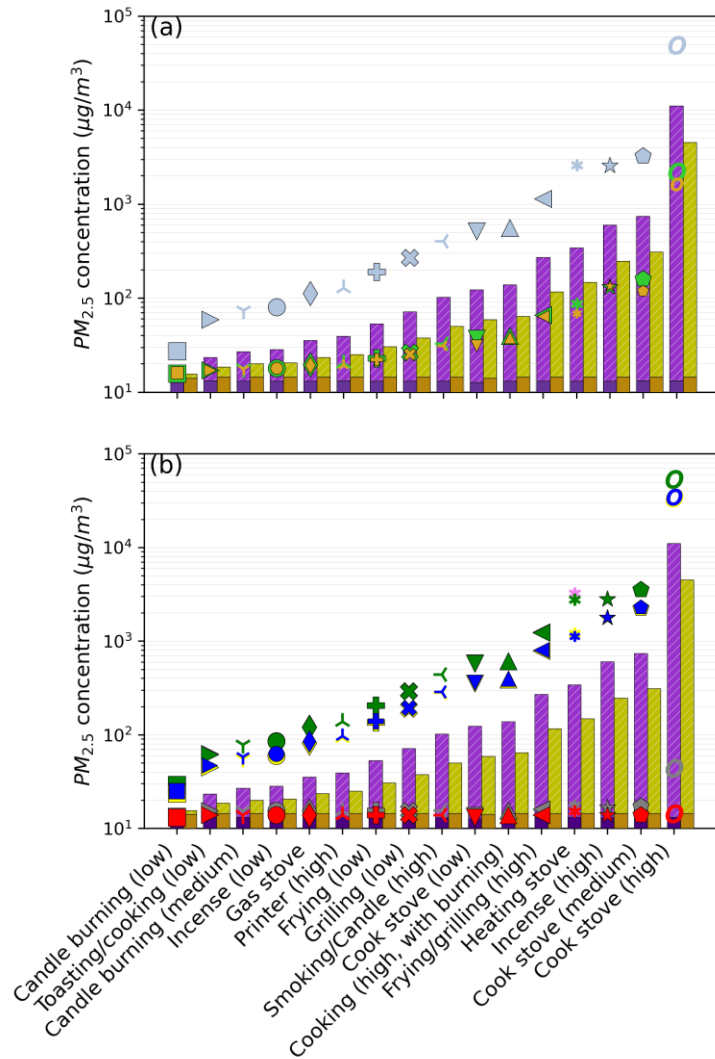
216 Figure 2: Indoor $PM_{2.5}$ concentrations from outdoors (navy) and increment from one hour
 217 activities (orange) over 24 hours: (a) toasting or cooking on an electric stove, (b) grilling
 218 (low), (c) smoking or lighting a candle with essential oil diffusion and (d) coal heating stove.

219 $PM_{2.5}$ concentration increments are higher for higher emission rates: the use of a coal
 220 heating stove can lead to a peak of $4500 \mu\text{g}/\text{m}^3$, while toasting or cooking on an electric stove
 221 lead to a peak of $150 \mu\text{g}/\text{m}^3$. The area under the curve gives the concentration to which
 222 occupants are exposed over a given duration ($\mu\text{g}\cdot\text{s}/\text{m}^3$), which is important to consider in health
 223 impact assessment. It is ultimately linked to the decay rate, mainly determined by the air change
 224 rate: higher ACH lead to higher decay rates.

225 24-h average concentrations for the different activities and ventilation scenarios,
 226 calculated from results of the dynamic model, are presented in Figure 3 for the room with small
 227 volume/high occupancy HO of $30 \text{ m}^3/\text{occupant}$. Concentrations in the room with higher

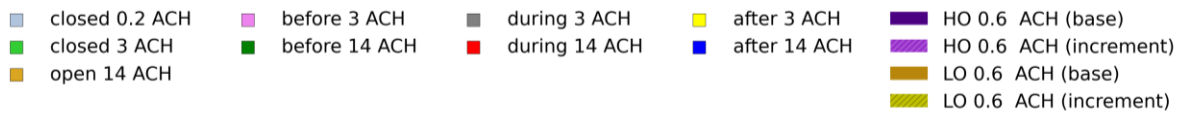
228 volume/low occupancy LO of $67 \text{ m}^3/\text{occupant}$ correspond to the average ventilation rate of
 229 0.6 ACH.

230



231

232



233

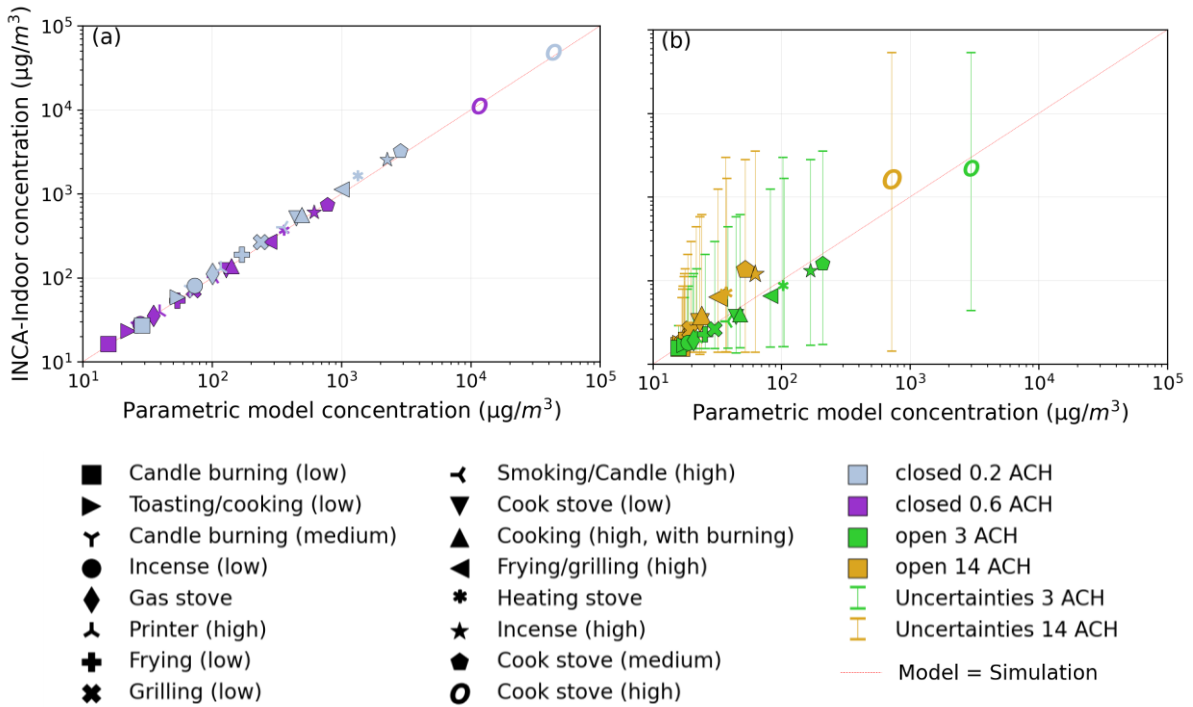
234 Figure 3: Bars represent $PM_{2.5}$ concentrations for an average scenario with 0.6 ACH without
 235 indoor emission (*base*) and with emissions from activities (*increment*) for a room with small
 236 volume and high occupancy (*HO*) and a room with high volume and low occupancy (*LO*).

237 Markers represent concentrations for (a) three other ACH in the small room: 0.2 ACH
 238 (always **closed**), 3 ACH and 14 ACH (always **open**) and (b) two ACH: 3 ACH and 14 ACH
 239 for different opening scenarios (open **before**, open **during** and open **after**)

240 The increment in the larger room is on average 2.5 times lower than that in the smaller
241 room, and the ratio of their volumes is 2.2. The difference can be explained by a higher
242 deposition rate in the larger room due to larger available surface area. Higher ventilation rates
243 lead to a decrease in concentrations if windows are always open or closed. We note from the
244 other scenarios presented in [Figure 3 \(b\)](#), that least concentrations are linked to opening
245 windows during the activity, since ventilation rates during emission are much higher, while
246 opening before the activity does not affect concentrations: they are equal to the closed window
247 scenario. Opening after the activity allows for partial evacuation of substances and hence a
248 slight decrease in concentrations (see SI Figure S2).

249 **3.2. Parametric model indoor PM_{2.5} concentrations**

250 The average PM_{2.5} concentration over 24 hours are calculated for each activity with the
251 parametric model described by equation (4). Though the parametric model with a mean ACH
252 throughout the day can provide a good estimation of 24-h average indoor air concentrations
253 (e.g. for fixed mechanical ventilation), under certain conditions, the dynamic model is more
254 precise. In most cases, the ACH changes throughout the day according to opening/closing of
255 windows and meteorological conditions. The latter determines natural air flow rates through
256 openings and infiltration. If variations in ACH occur during or right after emissions, indoor
257 PM_{2.5} concentrations are affected. The different scenarios are illustrated with error bars in
258 [Figure 4](#).



259

260

261 Figure 4: INCA-Indoor v/s parametric model 24-h average indoor PM2.5 concentrations
 262 from different activities for (a) **closed** windows at 0.2 and 0.6 ACH and (b) air renewal of 3
 263 and 14 ACH for windows always **open**, and uncertainties linked to window opening scenarios

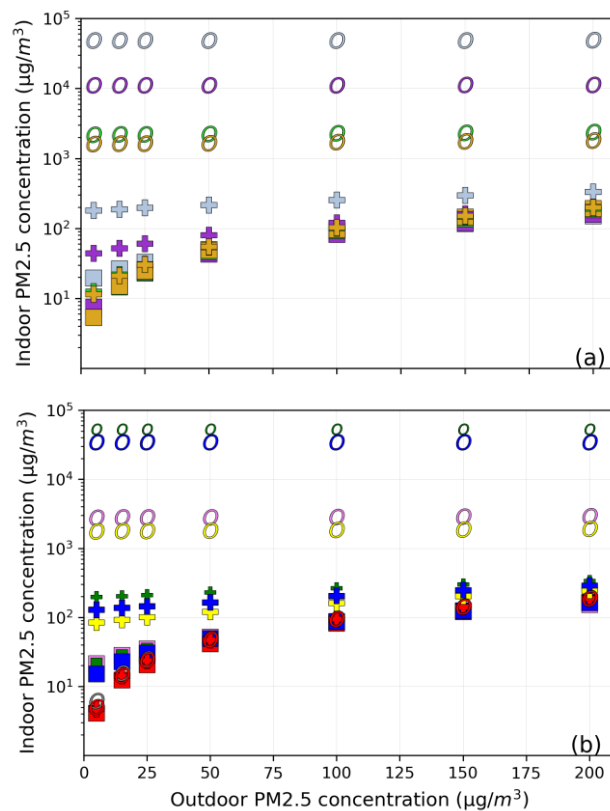
264 Activities in airtight buildings with windows closed (0.2 ACH) or open before the
 265 activity lead to the highest concentrations. In Figure 4 (a), we note that there is no uncertainty
 266 bar related to scenarios with 0.2 and 0.6 ACH since windows are considered to be closed. In
 267 scenarios with 3 and 14 ACH, windows can be always open, or open before, during or after the
 268 activity. Lowest concentrations (lower end of the error bar) correspond to scenarios where
 269 windows are open during the emission, evacuating almost all emitted particles and leading to a
 270 concentration approximately equal to \bar{C}_{out} . Highest concentrations are linked to windows
 271 always being closed, with an infiltration rate of 0.2 ACH, or scenarios where the windows are
 272 open before the activity, hence not affecting activity-related concentrations. The uncertainty
 273 factors between the parametric model and the dynamic simulation, based on the root mean
 274 squared log of error (RMSLE), are 1.18, 1.00, 1.03 and 1.14 for the following scenarios
 275 respectively: closed window at 0.2 ACH and 0.6 ACH and window always open at 3 ACH and
 276 14 ACH. The average percentage error is <3%. The uncertainties are linked to the variations in

277 ACH due to meteorological conditions affecting natural ventilation rates, which are not
 278 considered by the parametric model (see SI Figure S2).

279 **3.3. Contribution of outdoor PM_{2.5} level on indoor concentrations**

280 Dynamic and parametric model concentrations were calculated for an average European
 281 city with an average background PM_{2.5} level of 16 µg/m³, while, for different cities in the world,
 282 outdoor PM_{2.5} concentrations can range from 4 µg/m³ to 200 µg/m³ [46]. Figure 5 illustrates
 283 the effect of different outdoor PM_{2.5} levels on indoor concentrations for different ventilation
 284 scenarios and three activities representing low, medium and high emission rates: candle burning
 285 (low), frying (low) and cook stove (high).

286



287

- Candle burning (low) □ closed 0.2 ACH ■ open 3 ACH ■ before 3 ACH ■ during 3 ACH ■ after 3 ACH
- ⊕ Frying (low) ■ closed 0.6 ACH ■ open 14 ACH ■ before 14 ACH ■ during 14 ACH ■ after 14 ACH
- Cook stove (high)

288

289 Figure 5: Indoor PM_{2.5} concentrations for three different activities and seven outdoor
 290 concentrations (4 – 200 µg/m³) for a) four standard ACH: (a) 0.2 ACH and 0.6 ACH with
 291 **closed** windows and 3 ACH and 14 ACH with windows **always** open, and (b) 3 ACH or
 292 14 ACH for different opening scenarios (open **before**, open **during** and open **after**)

293 We note from Figure 5 that, for activities with high emissions such as incense burning,
294 outdoor concentrations have low relative effect on indoor concentrations (only up to 6%
295 increase), while they can lead to an 8-fold increase for low-emission activities such as candle
296 burning (low). At very high outdoor concentrations and for low emission rates such as candle
297 burning, average concentrations are lower for closed window scenarios since the highest
298 contribution to indoor $PM_{2.5}$ is outdoor air.

299 **3.4. Intake fractions, effect factors and characterisation factors for different indoor** 300 **activities**

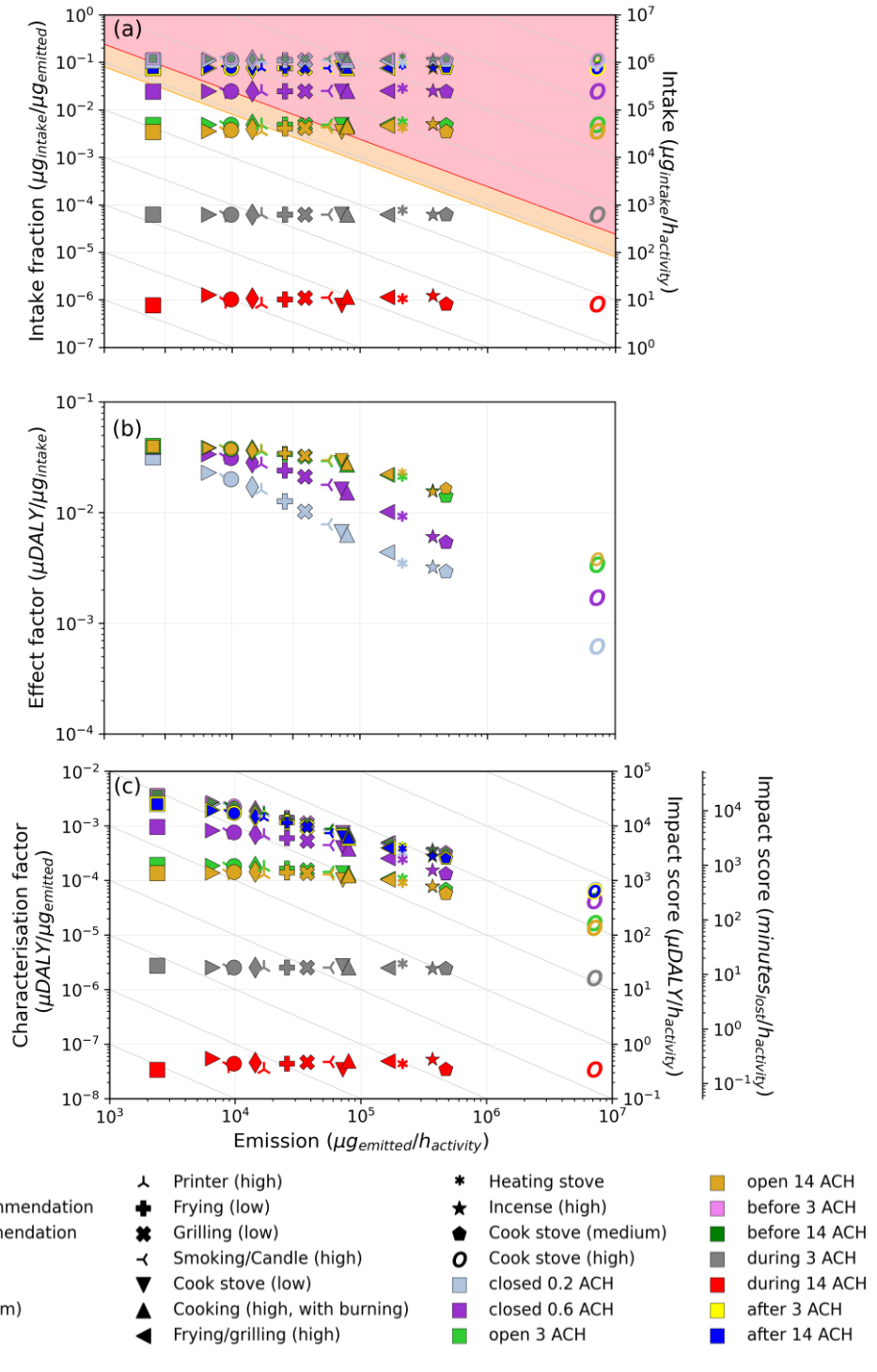
301 Intake quantities and impacts for each activity are calculated **per occupant and per**
302 **hour** of activity. The uncertainty factors for the intake mass (μg) calculated by the parametric
303 versus the dynamic model are 1.0, 1.05, 1.04 and 1.37, respectively, for the standard scenarios
304 with 0.2, 0.6, 3 and 14 ACH.

305 Intake fractions ($\mu\text{g}_{\text{intake}}/\mu\text{g}_{\text{emitted}}$) and intake rates ($\mu\text{g}_{\text{intake}}/h_{\text{activity}}$) calculated using the
306 dynamic concentrations for all activities and ventilation scenarios are shown in [Figure 6 \(a\)](#).
307 Orange and red lines represent the annual and daily exposure recommendations from the WHO
308 air quality guidelines respectively [8]. [Figure 6 \(b\)](#) shows effect factors ($\mu\text{DALY}/\mu\text{g}_{\text{intake}}$) for
309 all activities and four standard ventilation scenarios, and [Figure 6 \(c\)](#) shows characterisation
310 factors ($\mu\text{DALY}/\mu\text{g}_{\text{emitted}}$) on the primary y-axis and impact scores ($\mu\text{DALY}/h_{\text{activity}}$ and
311 $\text{minutes}_{\text{lost}}/h_{\text{activity}}$) on the secondary y-axes with diagonal iso-impact lines for all activities and
312 scenarios.

313

314

315



316

317

318

319

320

321

322

323

Figure 6: a) Intake fractions ($\mu\text{g}_{\text{intake}}/\mu\text{g}_{\text{emitted}}$) for all activities and ventilation scenarios on the primary y-axis and total intake ($\mu\text{g}_{\text{intake}}/h_{\text{activity}}$) on the secondary y-axis, with iso-intake diagonal lines in grey and annual and daily recommendations represented by yellow and red lines, (b) effect factors ($\mu\text{DALY}/\mu\text{g}_{\text{intake}}$) for all activities and four standard ventilation scenarios and (c) characterisation factors ($\mu\text{DALY}/\mu\text{g}_{\text{emitted}}$) on the primary y-axis and health damages ($\mu\text{DALY}/h_{\text{activity}}$ and minutes_{lost}/d) on the two secondary y-axes (left and right) with iso-impact diagonal lines in grey.

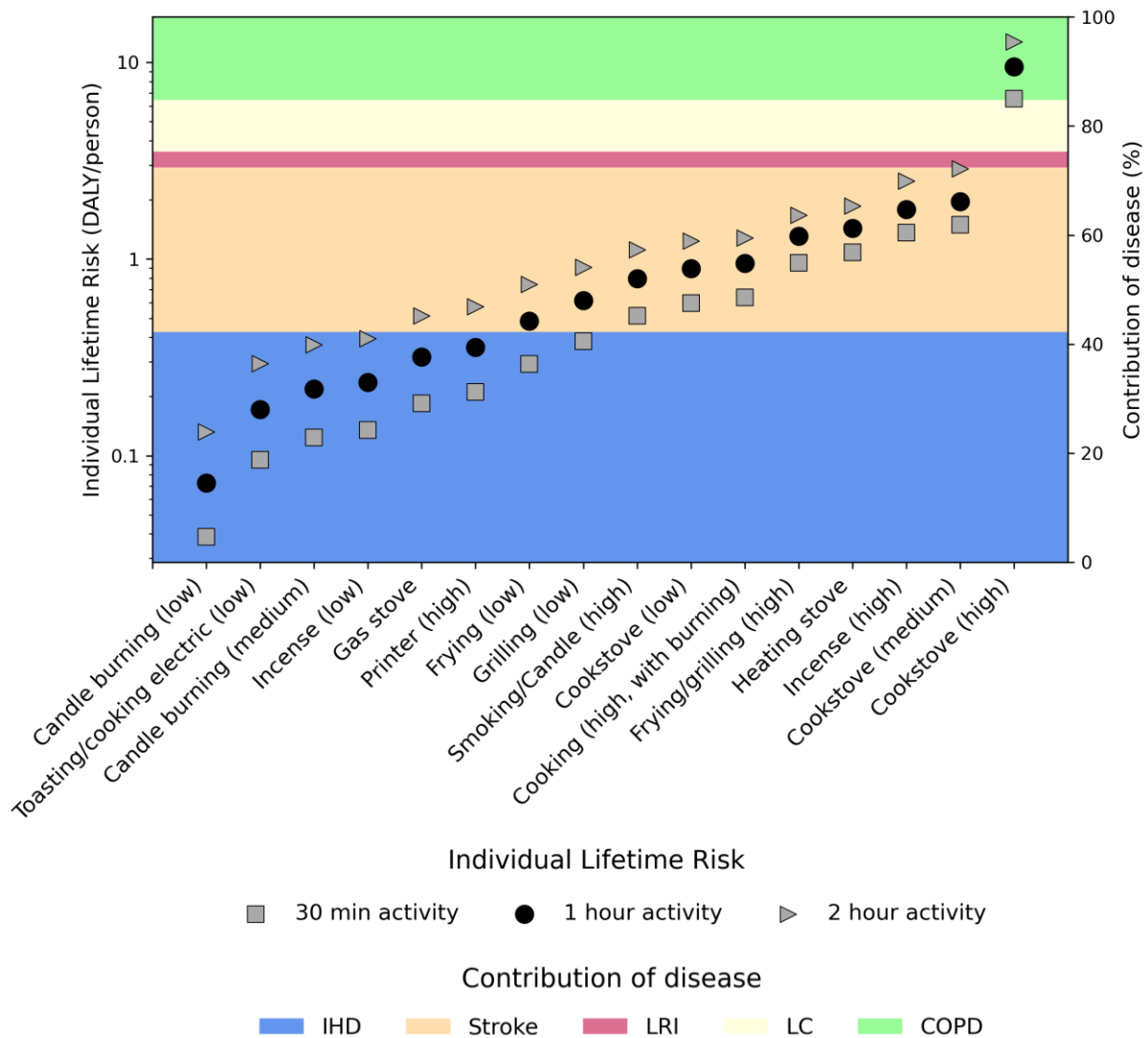
324 Intake fractions ($\mu\text{g}_{\text{intake}}/\mu\text{g}_{\text{emitted}}$) calculated by equation (2) are different for each
325 scenario but independent of the emission rate: they depend on breathing rate, occupancy,
326 particle deposition rate and ACH [4]. Given a ventilation scenario, the total intake
327 ($\mu\text{g}_{\text{intake}}/h_{\text{activity}}$), represented by diagonal grey iso-intake lines, is higher for activities with
328 higher emission rates. Markers in the orange and red zone indicate activity and window-opening
329 combinations that lead to concentrations, and consequently intake quantities, beyond WHO
330 guidelines. These include low-emission activities such as lighting a candle in a closed airtight
331 building at 0.2 ACH, which is a possible scenario. Unless having a very high ventilation rate
332 (windows open only during activity, with a 24-hour average of 14 ACH) during the use of a
333 very high-emission cook stove, all scenarios lead to intake well above guidelines.

334 Figure 6 (b) shows that effect factors decrease with increasing emission rate for each
335 scenario, since they depend on indoor $\text{PM}_{2.5}$ concentrations. Characterisation factors CF ,
336 product of iF and EF , also vary across activities and scenarios (see Figure 6 (c)). Least impacts
337 occur when windows are open during activities, especially if ventilation rates are very high (e.g.
338 with cross ventilation). We also note that indoor fuel burning for cooking (high, using maize
339 straw) can lead to very high health impacts of $484 \mu\text{DALY}/h_{\text{activity}}$ (about 4 $\text{hours}_{\text{lost}}$) in closed
340 buildings at 0.2 ACH. However, these ACH are unlikely for this activity, occurring in rural
341 homes in buildings with potentially high infiltration rates. Furthermore, occupants might
342 ventilate during the use of the cook stove, which can otherwise cause discomfort due to
343 increased temperatures and high, perceptible, $\text{PM}_{2.5}$ levels. Air renewal rates are more likely to
344 be around 3 to 14 ACH, resulting in 98 to $119 \mu\text{DALY}/h_{\text{activity}}$ (52 to 63 $\text{minutes}_{\text{lost}}/h_{\text{activity}}$). On
345 the other hand, candle burning can potentially occur in airtight buildings with closed windows,
346 at 0.2 or 0.6 ACH, leading to 7 to $20 \mu\text{DALY}/h_{\text{activity}}$ (4 to 11 $\text{minutes}_{\text{lost}}/h_{\text{activity}}$).

347 For a given activity-window scenario combination in the larger room (67 m³),
348 concentrations are lower (see [Figure 3](#)), impact scores are also lower. Results for the larger
349 room are given in SI.

350 **3.5. Individual lifetime risk**

351 The individual lifetime risk (*ILR*) (DALY/person), representing the number of life years
352 lost from the five disease outcomes, are calculated for each activity for an average scenario of
353 0.6 ACH air change rate from equation (6) and illustrated in Figure 7. It is considered that an
354 individual is exposed PM_{2.5} resulting from daily one-hour activities over a lifetime of 86 years
355 [47]. The ILR for 30-minute and 2-hour activity durations are also given.



356

357

358 Figure 7: Total individual lifetime risks (DALY/person) given by black markers for one-hour
 359 activities at 0.6 ACH and grey markers for 30-minute and two-hour durations on the left y-
 360 axis, with contributions of each disease (ischaemic heart disease *IHD*, stroke, lower
 361 respiratory infections *LRI*, lung cancer *LC* and chronic obstructive pulmonary disease *COPD*)
 362 given on the right y-axis

363

364

365

Activities with very high emissions can lead to a loss of up to 10 years of life, distributed
 as follows for the use of cook stove (high): 42% of the risk is related to *IHD*, 30% to stroke,
 3% to *LRI*, 9% to *LC* and 15% to *COPD*.

366

367

368

From Figure 7, we note variations in the distance between the ILR for the default activity
 duration (one hour) and that of each two additional durations (30 minutes and 2 hours) for
 different activities. These are explained by two non-linearities, one associated with the effect

369 factor and one associated with the intake. First, the exposure-response model underlying the
370 effect factors is supra-linear and dependent on indoor $PM_{2.5}$ concentrations (see equation 3),
371 which are a function of both indoor activity emissions and outdoor $PM_{2.5}$ levels. Second, intake
372 considers the concentration increment associated with a specific activity, and is hence non-
373 linearly dependent on indoor $PM_{2.5}$ concentrations (especially at very low emission rates, where
374 outdoor $PM_{2.5}$ have a higher relative influence on indoor $PM_{2.5}$ concentrations).

375 **3.6. Discussion**

376 We have seen that the parametric model can be used with little or no variation in ACH
377 during the day, but cannot integrate dynamic ventilation or occupancy scenarios. As for the
378 dynamic model, window-opening scenarios can be defined with a minimum of one-hour time
379 steps, while in reality, occupants can open windows for only a few minutes, especially during
380 cold weather. Ventilation durations are thus potentially overestimated, leading to
381 underestimations in concentrations and impacts, in particular for the *open during* and *open after*
382 scenarios.

383 In the particular case of the heating stove, opening windows during the activity is
384 counterproductive, leading to higher heating needs and thus higher environmental impacts.
385 With a life cycle perspective, it is thus important to consider heating as a source of impacts
386 (calculated using an energy simulation and LCA software) and identify best trade-offs that
387 allow to reduce damages from $PM_{2.5}$ and heating altogether.

388 The emission factor obtained in literature is dependent on the mass of coal burnt [23],
389 which was calculated according to heating needs with Pleiades [36]. The emission rate could
390 thus be adapted in the model if specific information on the mass burnt or heating need is known.
391 Furthermore, activities linked with indoor burning of fuels are more likely to occur in rural
392 regions, in homes having high ventilation/infiltration rates. Different ventilation rates can be
393 used as sensitivity analysis to reflect associations between indoor pollution levels and occupant

394 behaviour (e.g. opening of windows when concentrations are uncomfortably high), especially
395 if actual ventilation rates are unknown. In an LCA context, results are given for a large number
396 of scenarios that combine different emission rates and building characteristics (i.e. ventilation
397 rates and occupancy). Practitioners can thus apply those results that are relevant for their
398 specific study context.

399 Health impacts are calculated for activities with a reference duration of one hour, but
400 some activities can be shorter (e.g. smoking for a few minutes) or last longer (e.g. heating for a
401 few hours). Scaling results to actual activity durations can provide approximations, since the
402 calculated non-linear effect factors depend on average indoor air PM_{2.5} concentrations, which
403 vary with different activity durations. A sensitivity analysis is given in SI section S.6. for the
404 duration of 30 minutes and 2 hours for all activities at 0.6 ACH. Similarly, the factors provided
405 do not consider multiple occurrences of different activities at the same time, which could
406 increase concentrations and lead to variations in effect factors and impact scores. Finally, the
407 emission of other contaminants from the activities (e.g. volatile organic compounds, VOCs,
408 from candle burning) were not considered, which could be responsible for additional health
409 impacts.

410 Future scopes include the study of the influence of PM toxicity if compositions of
411 emitted particles for specific activities are known, and the calculation of characterisation factors
412 and impact scores for more activities. Studies focusing on fugitive emissions are few and fairly
413 recent. With growing awareness around health impacts of indoor solid fuel burning for heating
414 or cooking, more data could be available and allow to derive impact scores for different types
415 of stoves (e.g. certified heating stoves). The effect of a kitchen hood, which lead to 60 to 100%
416 reduction in PM_{2.5} concentrations [48], on health impacts of cooking could be included.
417 Furthermore, effect factors were calculated based on ambient PM_{2.5} concentrations, though
418 occupants are mainly exposed to indoor concentrations, which are often higher than outdoors:

419 effect factors are hence possibly overestimated. Representative building archetypes with their
420 respective activity scenarios can be modelled to calculate annual exposure concentrations
421 considering the fractions of time spent indoors and outdoors.

422 **4. Conclusion**

423 In this paper, we have provided a set of intake fractions, effect factors, characterisation
424 factors and impact scores for 19 one-hour activities and 10 different ventilation scenarios.
425 Indoor concentrations depend on indoor settings (e.g. window layout and opening scenarios),
426 outdoor PM_{2.5} level and activity duration. These parameters influence the indoor exposure
427 PM_{2.5} level used to calculate effect factors. We note that, at very low ACH, all activities induced
428 exposure concentrations beyond WHO recommendations. High or very high ventilation *during*
429 all activities allowed to reduce concentrations well below these recommendations. For instance,
430 98 to 119 $\mu\text{DALY}/h_{\text{activity}}$ (52 to 63 $\text{minutes}_{\text{lost}}/h_{\text{activity}}$) were associated with traditional fuel cook
431 stoves, with high air renewal rates (3 and 14 ACH), while 7 to 11 $\mu\text{DALY}/h_{\text{activity}}$ (4 to
432 11 $\text{minutes}_{\text{lost}}/h_{\text{activity}}$) were associated with candle burning in closed buildings at 0.2 to
433 0.6 ACH. Characterisation factors for the one-hour activities (or any other activities with
434 corresponding emission rates) provided in this study can be integrated to LCIA methods and
435 the framework proposed can help to devise optimal ventilation strategies in building design.
436 The derived impact scores ($CF \times ER_{\text{activity}}$) for an activity unit of one hour can be scaled by
437 activity duration to obtain an approximation of actual activity impacts. This constitutes a
438 valuable starting point for the integration of indoor activities and their PM_{2.5}-related emissions,
439 exposures and health effects into LCA and environmental footprint studies.

440 **Acknowledgements**

441 The authors would like to thank the financial support by the Chair ParisTech VINCI
442 Eco-design of buildings and infrastructure. The project acknowledges the UNEP GLAM project
443 human health task force, and the financial support from the USEtox International Centre.

444 **Supplementary description**

445 In Supplementary Material 1, background model data, ventilation scenario descriptions,
446 heat stove emission calculations, the particle size number distribution, indoor PM_{2.5}
447 concentrations as a function of ventilation scenario and results for the larger room are provided.
448 In Supplementary Material 2, effect factors, characterisation factors and impact scores for all
449 activities, scenarios and occupancy rates are given.

450 **References**

- 451 [1] Murray CJL, Aravkin AY, Zheng P, Abbafati C, Abbas KM, Abbasi-Kangevari M, et al.
452 Global burden of 87 risk factors in 204 countries and territories, 1990–2019: a systematic
453 analysis for the Global Burden of Disease Study 2019. *The Lancet* 2020;396:1223–49.
454 [https://doi.org/10.1016/S0140-6736\(20\)30752-2](https://doi.org/10.1016/S0140-6736(20)30752-2).
- 455 [2] Burnett RT, Pope CA, Ezzati M, Olives C, Lim SS, Mehta S, et al. An Integrated Risk
456 Function for Estimating the Global Burden of Disease Attributable to Ambient Fine
457 Particulate Matter Exposure. *Environmental Health Perspectives* 2014;122:397–403.
458 <https://doi.org/10.1289/ehp.1307049>.
- 459 [3] Fantke P, Jolliet O, Evans JS, Apte JS, Cohen AJ, Hänninen OO, et al. Health effects of
460 fine particulate matter in life cycle impact assessment: findings from the Basel Guidance
461 Workshop. *Int J Life Cycle Assess* 2015;20:276–88. <https://doi.org/10.1007/s11367-014-0822-2>.
- 462
463 [4] Fantke P, Jolliet O, Apte JS, Hodas N, Evans J, Weschler CJ, et al. Characterizing
464 Aggregated Exposure to Primary Particulate Matter: Recommended Intake Fractions for
465 Indoor and Outdoor Sources. *Environ Sci Technol* 2017;51:9089–100.
466 <https://doi.org/10.1021/acs.est.7b02589>.
- 467 [5] OQAI. Une campagne nationale pour évaluer la qualité des environnements intérieurs des
468 écoles françaises 2018. [https://www.oqai.fr/fr/campagnes/campagne-nationale-ecoles-](https://www.oqai.fr/fr/campagnes/campagne-nationale-ecoles-n01)
469 [n01](https://www.oqai.fr/fr/campagnes/campagne-nationale-ecoles-n01) (accessed May 29, 2023).
- 470 [6] Mandin C. The Indoor Air Quality Observatory (OQAI): a unique project to understand
471 air pollution in our living spaces. *Field Actions Science Reports The Journal of Field*
472 *Actions* 2020:18–23.
- 473 [7] Mainka A, Fantke P. Preschool children health impacts from indoor exposure to PM2.5
474 and metals. *Environment International* 2022;160:107062.
475 <https://doi.org/10.1016/j.envint.2021.107062>.
- 476 [8] WHO. WHO global air quality guidelines: particulate matter (PM2.5 and PM10), ozone,
477 nitrogen dioxide, sulfur dioxide and carbon monoxide. World Health Organization; 2021.
- 478 [9] Smith KR. National burden of disease in India from indoor air pollution. *Proceedings of*
479 *the National Academy of Sciences* 2000;97:13286–93.
480 <https://doi.org/10.1073/pnas.97.24.13286>.
- 481 [10] Smith KR, McCracken JP, Weber MW, Hubbard A, Jenny A, Thompson LM, et al. Effect
482 of reduction in household air pollution on childhood pneumonia in Guatemala
483 (RESPIRE): a randomised controlled trial. *The Lancet* 2011;378:1717–26.
484 [https://doi.org/10.1016/S0140-6736\(11\)60921-5](https://doi.org/10.1016/S0140-6736(11)60921-5).
- 485 [11] Rohra H, Tiwari R, Khandelwal N, Taneja A. Mass distribution and health risk assessment
486 of size segregated particulate in varied indoor microenvironments of Agra, India - A case
487 study. *Urban Climate* 2018;24:139–52. <https://doi.org/10.1016/j.uclim.2018.01.002>.
- 488 [12] Srivastava D, Vu TV, Tong S, Shi Z, Harrison RM. Formation of secondary organic
489 aerosols from anthropogenic precursors in laboratory studies. *Npj Clim Atmos Sci*
490 2022;5:1–30. <https://doi.org/10.1038/s41612-022-00238-6>.

- 491 [13] Isaxon C, Gudmundsson A, Nordin EZ, Lönnblad L, Dahl A, Wieslander G, et al.
492 Contribution of indoor-generated particles to residential exposure. *Atmospheric*
493 *Environment* 2015;106:458–66. <https://doi.org/10.1016/j.atmosenv.2014.07.053>.
- 494 [14] He C, Morawska L, Hitchins J, Gilbert D. Contribution from indoor sources to particle
495 number and mass concentrations in residential houses. *Atmospheric Environment*
496 2004;38:3405–15. <https://doi.org/10.1016/j.atmosenv.2004.03.027>.
- 497 [15] Pagels J, Wierzbicka A, Nilsson E, Isaxon C, Dahl A, Gudmundsson A, et al. Chemical
498 composition and mass emission factors of candle smoke particles. *Journal of Aerosol*
499 *Science* 2009;40:193–208. <https://doi.org/10.1016/j.jaerosci.2008.10.005>.
- 500 [16] Aquilina NJ, Camilleri SF. Impact of daily household activities on indoor PM_{2.5} and
501 Black Carbon concentrations in Malta. *Building and Environment* 2022;207:108422.
502 <https://doi.org/10.1016/j.buildenv.2021.108422>.
- 503 [17] Long CM, Suh HH, Koutrakis P. Characterization of Indoor Particle Sources Using
504 Continuous Mass and Size Monitors. *Journal of the Air & Waste Management Association*
505 2000;50:1236–50. <https://doi.org/10.1080/10473289.2000.10464154>.
- 506 [18] He C, Morawska L, Hitchins J, Gilbert D. Contribution from indoor sources to particle
507 number and mass concentrations in residential houses. *Atmospheric Environment*
508 2004;38:3405–15. <https://doi.org/10.1016/j.atmosenv.2004.03.027>.
- 509 [19] Tissari J, Lyyräinen J, Hytönen K, Sippula O, Tapper U, Frey A, et al. Fine particle and
510 gaseous emissions from normal and smouldering wood combustion in a conventional
511 masonry heater. *Atmospheric Environment* 2008;42:7862–73.
512 <https://doi.org/10.1016/j.atmosenv.2008.07.019>.
- 513 [20] Shen G, Du W, Luo Z, Li Y, Cai G, Lu C, et al. Fugitive Emissions of CO and PM_{2.5}
514 from Indoor Biomass Burning in Chimney Stoves Based on a Newly Developed Carbon
515 Balance Approach. *Environ Sci Technol Lett* 2020;7:128–34.
516 <https://doi.org/10.1021/acs.estlett.0c00095>.
- 517 [21] Demanega I, Mujan I, Singer BC, Anđelković AS, Babich F, Licina D. Performance
518 assessment of low-cost environmental monitors and single sensors under variable indoor
519 air quality and thermal conditions. *Building and Environment* 2021;187:107415.
520 <https://doi.org/10.1016/j.buildenv.2020.107415>.
- 521 [22] Du W, Zhuo S, Wang J, Luo Z, Chen Y, Wang Z, et al. Substantial leakage into indoor air
522 from on-site solid fuel combustion in chimney stoves. *Environmental Pollution*
523 2021;291:118138. <https://doi.org/10.1016/j.envpol.2021.118138>.
- 524 [23] Li C, Ye K, Zhang W, Xu Y, Xu J, Li J, et al. User behavior, influence factors, and impacts
525 on real-world pollutant emissions from the household heating stoves in rural China.
526 *Science of The Total Environment* 2022;823:153718.
527 <https://doi.org/10.1016/j.scitotenv.2022.153718>.
- 528 [24] Ferro AR, Kopperud RJ, Hildemann LM. Source Strengths for Indoor Human Activities
529 that Resuspend Particulate Matter. *Environ Sci Technol* 2004;38:1759–64.
530 <https://doi.org/10.1021/es0263893>.
- 531 [25] Corsi RL, Siegel JA, Chiang C. Particle Resuspension During the Use of Vacuum Cleaners
532 on Residential Carpet. *Journal of Occupational and Environmental Hygiene* 2008;5:232–
533 8. <https://doi.org/10.1080/15459620801901165>.

- 534 [26] Bhangar S, Adams RI, Pasut W, Huffman JA, Arens EA, Taylor JW, et al. Chamber
535 bioaerosol study: human emissions of size-resolved fluorescent biological aerosol
536 particles. *Indoor Air* 2016;26:193–206. <https://doi.org/10.1111/ina.12195>.
- 537 [27] Licina D, Tian Y, Nazaroff WW. Emission rates and the personal cloud effect associated
538 with particle release from the perihuman environment. *Indoor Air* 2017;27:791–802.
539 <https://doi.org/10.1111/ina.12365>.
- 540 [28] Al Assaad D, Ghali K, Ghaddar N, Shammass E. Modeling of indoor particulate matter
541 deposition to occupant typical wrinkled shirt surface. *Building and Environment*
542 2020;179:106965. <https://doi.org/10.1016/j.buildenv.2020.106965>.
- 543 [29] Hodas N, Loh M, Shin H-M, Li D, Bennett D, McKone TE, et al. Indoor inhalation intake
544 fractions of fine particulate matter: review of influencing factors. *Indoor Air* 2016;26:836–
545 56. <https://doi.org/10.1111/ina.12268>.
- 546 [30] Mendez M, Blond N, Blondeau P, Schoemaeker C, Hauglustaine DA. Assessment of the
547 impact of oxidation processes on indoor air pollution using the new time-resolved INCA-
548 Indoor model. *Atmospheric Environment* 2015;122:521–30.
549 <https://doi.org/10.1016/j.atmosenv.2015.10.025>.
- 550 [31] Humbert S, Marshall JD, Shaked S, Spadaro JV, Nishioka Y, Preiss P, et al. Intake
551 Fraction for Particulate Matter: Recommendations for Life Cycle Impact Assessment.
552 *Environ Sci Technol* 2011;45:4808–16. <https://doi.org/10.1021/es103563z>.
- 553 [32] Cohen AJ, Brauer M, Burnett R, Anderson HR, Frostad J, Estep K, et al. Estimates and
554 25-year trends of the global burden of disease attributable to ambient air pollution: an
555 analysis of data from the Global Burden of Diseases Study 2015. *The Lancet*
556 2017;389:1907–18. [https://doi.org/10.1016/S0140-6736\(17\)30505-6](https://doi.org/10.1016/S0140-6736(17)30505-6).
- 557 [33] Fantke P, McKone TE, Tainio M, Jolliet O, Apte JS, Stylianou KS, et al. Global Effect
558 Factors for Exposure to Fine Particulate Matter. *Environ Sci Technol* 2019;53:6855–68.
559 <https://doi.org/10.1021/acs.est.9b01800>.
- 560 [34] Lee S-C, Wang B. Characteristics of emissions of air pollutants from burning of incense
561 in a large environmental chamber. *Atmospheric Environment* 2004;38:941–51.
562 <https://doi.org/10.1016/j.atmosenv.2003.11.002>.
- 563 [35] He C, Morawska L, Wang H, Jayaratne R, McGarry P, Richard Johnson G, et al.
564 Quantification of the relationship between fuser roller temperature and laser printer
565 emissions. *Journal of Aerosol Science* 2010;41:523–30.
566 <https://doi.org/10.1016/j.jaerosci.2010.02.015>.
- 567 [36] IZUBA ÉNERGIES. Logiciel Pleiades. IZUBA ÉNERGIES 2001.
568 <https://www.izuba.fr/logiciels/outils-logiciels/> (accessed June 7, 2022).
- 569 [37] Biesebeek JD te, Nijkamp MM, Bokkers BGH, Wijnhoven SWP. Room size and
570 ventilation. General Fact Sheet: General default parameters for estimating consumer
571 exposure: Updated version 2014 [Internet], National Institute for Public Health and the
572 Environment; 2014.
- 573 [38] Pereira PF, Ramos NMM, Ferreira A. Room-scale analysis of spatial and human factors
574 affecting indoor environmental quality in Porto residential flats. *Building and*
575 *Environment* 2020;186:107376. <https://doi.org/10.1016/j.buildenv.2020.107376>.
- 576 [39] Kumar P, Hama S, Abbass RA, Nogueira T, Brand VS, Wu H-W, et al. CO₂ exposure,
577 ventilation, thermal comfort and health risks in low-income home kitchens of twelve

578 global cities. *Journal of Building Engineering* 2022;61:105254.
579 <https://doi.org/10.1016/j.jobbe.2022.105254>.

580 [40] Abt E, Suh HH, Catalano P, Koutrakis P. Relative Contribution of Outdoor and Indoor
581 Particle Sources to Indoor Concentrations. *Environ Sci Technol* 2000;34:3579–87.
582 <https://doi.org/10.1021/es990348y>.

583 [41] Rosenbaum RK, Meijer A, Demou E, Hellweg S, Jolliet O, Lam NL, et al. Indoor Air
584 Pollutant Exposure for Life Cycle Assessment: Regional Health Impact Factors for
585 Households. *Environ Sci Technol* 2015;49:12823–31.
586 <https://doi.org/10.1021/acs.est.5b00890>.

587 [42] Persily A, Musser A, Emmerich SJ. Modeled infiltration rate distributions for U.S.
588 housing. *Indoor Air* 2010;20:473–85. <https://doi.org/10.1111/j.1600-0668.2010.00669.x>.

589 [43] Aynsley R. Indoor Wind Speed Coefficients for Estimating Summer Comfort.
590 *International Journal of Ventilation* 2006;5:3–12.
591 <https://doi.org/10.1080/14733315.2006.11683719>.

592 [44] United Nations, Department of Economic and Social Affairs, Population Division. World
593 urbanization prospects: the 2018 revision. 2019.

594 [45] GBD Global Burden of Disease Collaborative Network. Global Burden of Disease Study
595 2019 (GBD 2019) Results. Institute for Health Metrics and Evaluation 2019.
596 <https://vizhub.healthdata.org/gbd-results> (accessed November 14, 2022).

597 [46] WHO. Modelled estimates of air pollution from particulate matter 2016.
598 [https://www.who.int/data/gho/data/themes/air-pollution/who-modelled-estimates-of-air-](https://www.who.int/data/gho/data/themes/air-pollution/who-modelled-estimates-of-air-pollution-from-particulate-matter)
599 [pollution-from-particulate-matter](https://www.who.int/data/gho/data/themes/air-pollution/who-modelled-estimates-of-air-pollution-from-particulate-matter) (accessed March 29, 2023).

600 [47] WHO. WHO methods and data sources for global burden of disease estimates 2000-2019
601 2020. [https://cdn.who.int/media/docs/default-source/gho-documents/global-health-](https://cdn.who.int/media/docs/default-source/gho-documents/global-health-estimates/gho2019_daly-methods.pdf?sfvrsn=31b25009_7)
602 [estimates/gho2019_daly-methods.pdf?sfvrsn=31b25009_7](https://cdn.who.int/media/docs/default-source/gho-documents/global-health-estimates/gho2019_daly-methods.pdf?sfvrsn=31b25009_7) (accessed May 4, 2023).

603 [48] Eom YS, Kang DH, Rim D, Yeo M. Particle dispersion and removal associated with
604 kitchen range hood and whole house ventilation system. *Building and Environment*
605 2023;230:109986. <https://doi.org/10.1016/j.buildenv.2023.109986>.

606

607